

Visualizing the perturbation of cellular cyclic di-GMP levels in bacterial cells

Ho, Chun Loong; Chong, Kavin Shi Jie; Oppong, Jamila Akosua; Chuah, Mary Lay-Cheng; Tan, Suet Mien; Liang, Zhao-Xun

2013

Ho, C. L., Chong, K. S. J., Oppong, J. A., Chuah, M. L. C., Tan, S. M., & Liang, Z. X. (2013). Visualizing the Perturbation of Cellular Cyclic di-GMP Levels in Bacterial Cells. *Journal of the American Chemical Society*, 135(2), 566-569.

<https://hdl.handle.net/10356/79909>

<https://doi.org/10.1021/ja310497x>

© 2013 American Chemical Society. This is the author created version of a work that has been peer reviewed and accepted for publication by *Journal of the American Chemical Society*, American Chemical Society. It incorporates referee's comments but changes resulting from the publishing process, such as copyediting, structural formatting, may not be reflected in this document. The published version is available at: [<http://dx.doi.org/10.1021/ja310497x>].

Downloaded on 20 Mar 2024 19:38:01 SGT

Visualizing the Perturbation of Cellular Cyclic di-GMP Levels in Bacterial Cells

Chun Loong Ho, Kavin Shi Jie Chong, Mary Lay Cheng Chuah, Suet Mien Tan, Zhao-Xun Liang*

Division of Structural Biology & Biochemistry, School of Biological Sciences, Nanyang Technological University, 60 Nanyang Drive, Singapore 637551.

Table of contents

Material and methods

Table S1 Test of the specificity of the biosensors by using the nucleotides from bacterial cells.

Table S2 Experimental concentrations of the biofilm-dispersing compounds and perturbation of FRET efficiencies in two *E. coli* strains.

Table S3 Minimal inhibition concentration (MIC), experimental concentrations of the antibiotics and perturbation of FRET efficiencies in two *E. coli* strains.

Fig. S1 In vitro characterization of cdg-S1 and cdg-S2 and cellular localization and fluorescent proteins.

Fig. S2 Perturbation of c-di-GMP levels in UTI89 *E. coli* cells by biofilm-dispersing agents as reported by Cdg-S1 and Cdg-S2.

Fig. S3 Perturbation of c-di-GMP levels in UTI89 *E. coli* cells by subinhibitory concentration antibiotics as reported by Cdg-S1 and Cdg-S2.

Fig. S4 Perturbation of c-di-GMP level in the UTI89 *E. coli* cells engulfed by macrophage as reported by Cdg-S1 and Cdg-S2.

Material and methods

Chemical and biological reagents

Top10 and BL21(DE3) *E. coli* cells were purchased from Invitrogen (Carlsbad, USA). The wild type uropathogenic *E. coli* strain UT189 was acquired as a gift from Drs. Liang Yang and Kimberley Kline (Nanyang Technological University, Singapore). Cyclic di-GMP and cyclic di-AMP were synthesized enzymatically in our laboratory. All the other chemicals, salt and buffer were purchased from Sigma-Aldrich (Steinheim, USA), Fluka (Steinheim, USA), USB (Cleveland, OH USA) and Merck (Darmstadt, Germany). All medium and ingredients were purchased from Bacton and other commercial sources.

Gene cloning, protein expression and purification

The genes that encode MrkH, VCA0042 and several other c-di-GMP binding proteins were cloned separately into the pET28 vector that harbors the mCerulean and mVenus genes. The DNA sequences that contain several restriction sites were designed to allow the optimization of the length of the linkers between the fluorescent protein genes and c-di-GMP binding protein gene. The resulting plasmids were transformed into *E. coli* BL21 (DE3) for protein expression and characterization. *E. coli* BL21(DE3) cells carrying the pET28 plasmids that harbor the biosensor constructs were grown in 5 mL Lysogeny Broth (LB) medium supplemented with 50 mg/L of kanamycin at 37 °C, 180 rpm overnight to prepare seeding culture. The seeding culture were then used to inoculate 800 mL of LB with 50 mg/L kanamycin; and the inoculated culture was allowed to grow under similar conditions as above until OD_{600nm} 0.6 ~ 0.8 Abs. The cultures were then cooled to 16 °C, induced with 0.5 mM Isopropyl β-D-1-thiogalactopyranoside (IPTG) and incubated at 16 °C, 160 rpm for 20 hours. Cells were harvested by centrifugation at 8,000 rpm for 10 minutes and re-suspended in 30 mL lysis buffer (50 mM NaH₂PO₄, 300 mM NaCl, 10% Glycerol and 1 mM dithiothreitol (DTT)). Cells were ruptured by passing the suspension through the Emulsiflex C3 Homogenizer equipped with cooling coil (Avestin, Canada) five times with a setting of 15 kPa. The lysate was then centrifuged at 20,000 rpm for 30 min (4 °C). Supernatant was incubated with Sephadex nickel-nitrilotriacetic acid (Ni-NTA) beads for one hour at 4 °C with gentle agitation before being loaded into a column. The beads were then washed with lysis buffer with a step gradient of imidazole-containing buffer (0 mM, 20 mM and

50 mM imidazole) and finally eluted with the elution buffer that contains 300 mM imidazole. The purity of eluted fractions was checked using 12% denaturing SDS-PAGE. The eluted fractions with the highest purity were pooled together and incubated with c-di-GMP phosphodiesterase RocR (with 10 mM MgCl₂) to remove the trace amount of c-di-GMP derived from the *E. coli* host cells. The incubation was performed in Snakeskin dialysis tubing with 10,000 MWCO, dialyzing against normal lysis buffer at 4 °C overnight to allow the maturation of mVenus. HPLC was employed to show that c-di-GMP bound to the biosensors was completely hydrolyzed to 5'-pGpG and GMP. The proteins were then further purified using gel-exclusion chromatography on an AKTA FPLC system equipped with a Superdex 200 HR 16/60 column (GE Healthcare). Pure protein fractions containing the unbound biosensor were then concentrated for storage and fluorescent titration assays described below.

In vitro fluorescence titration

C-di-GMP was prepared by enzymatic method as described previously¹. The purified FRET biosensor proteins were titrated with c-di-GMP to determine the effect of c-di-GMP binding on FRET efficiency and to determine the dissociation constants (K_d). Briefly, 250 nM of purified biosensors were titrated with c-di-GMP (0 ~ 12.5 μ M) in the 100 mM HEPES (pH 8.0) buffer. Fluorescence was measured by using a TECAN Infinite 200 PRO multi-plate reader with fluorescence measurement capabilities, with an excitation $\lambda_{433\text{ nm}}$ and scanning from 445 nm to 600 nm. The emission maxima of mCerulean and mVenus at 466 nm and 528 nm were monitored and the titration curves were plotted using the value of relative changes in emission ratio ($\text{Em}_{528\text{ nm}}/\text{Em}_{466\text{ nm}}$) against log [c-di-GMP]. The titration data were fitted to the one-site binding equations as shown below (**Eq. 1 and Eq. 2**).

$$[\text{c-di-GMP}] = K_d \cdot Q \cdot ((R - R_{\min}) / (R_{\max} - R)) \quad (\text{Eq. 1})$$

Where Q is the ratio of YFP/CFP emission and the lowest fluorescence emission (R_{\min}) and maximum emission (R_{\max}) represents the YFP/CFP emission ratio of the ligand-bound to unbound form.

$$Q = (P_1 \times [\text{c-di-GMP}]) / (K_d + [\text{c-di-GMP}]) + P_2 \quad (\text{Eq. 2})$$

Where Q is the ratio of YFP/CFP emission; P_1 is the ratiometric change upon c-di-GMP binding; P_2 is the YFP/CFP ratio in the absence of c-di-GMP. Similar results (K_d values) were obtained from the fitting to the two equations. To validate the specificity of the sensor, the sensors were also titrated with a set of naturally occurring nucleotides at physiologically relevant concentrations (Table S1). The concentrations of the nucleotides used were based on the reported values². From these experiments, Cdg-S1 and Cdg-S2 emerged as the best performers with significant changes in FRET efficiency upon c-di-GMP binding and little interference from other nucleotides.

Construction of the expression plasmids for the uropathogenic *E. coli* UTI89

The gene coding for Cdg-S2 was amplified by PCR by using the primers that contain XbaI and PstI restriction sites. The gene coding for Cdg-S1 was amplified by PCR by using the primers that contain XbaI and SmaI restriction sites. The amplified fragments were ligated into pUCP18 plasmid for constitutive protein expression in the wild type *E. coli* UTI89 strain via the P_{Lac} promoter³. This resulted pUCP18 plasmids that harbor the *cdg-S1* gene (pUCP18-*cdgS1*) and *cdg-S2* gene (pUCP18-*cdgS2*).

Transformation of the uropathogenic *E. coli* UTI89

The plasmids obtained above were transformed into the electro-competent UTI89 *E. coli* cells using 1.8 kV with a GenePulser Xcell (Biorad) and selected on LB agar plates with 100 mg/L ampicillin. Positive transformants were picked and used to inoculate the LB medium supplemented with 100 mg/L ampicillin for 20 hours at 37 °C. Prepared cells were transferred onto 1% agarose pads on a 15 well Multitest microscope slide (MP Biomedical, USA). Cells were then visualized using LSM510 Meta Confocal Microscope (Zeiss, Germany), using excitation 430 nm and 514 nm to validate the presence of both fluorescent proteins.

Perturbation of c-di-GMP levels in *E. coli* by subinhibitory concentrations of antibiotics

BL21 *E. coli* cells that express Cdg-S1 or Cdg-S2 biosensor were grown in LB medium supplemented with 50 mg/L kanamycin to about OD_{600nm} 0.6 ~ 0.8 at 37 °C, 180 rpm before being cooled down to 16 °C. Cultures were induced with 0.1 mM IPTG for 6 hours at 20 °C, 180

rpm before the cells were suspended in a 10 × diluted LB medium and incubated overnight at 4 °C with gentle rocking to allow mVenus maturation. Cell culture was then immediately changed into fresh warm LB medium without antibiotic before being subjected to antibiotic treatment. The biosensor-containing UTI89 *E. coli* cells were grown in LB medium supplemented with 100 mg/L of ampicillin to about OD_{600nm} 0.2 ~ 0.3 at 37 °C before being resuspended in fresh LB medium and allowed to grow at room temperature for 36 hours. Cells were subsequently resuspended in fresh warm LB medium to reach an OD_{600nm} of 0.6 ~ 0.8 by dilution before antibiotic treatment.

The *E. coli* cells were treated with antibiotics of sub-minimal inhibitory concentrations as indicated in **Table S3**. The individual antibiotics were added separately to cell cultures and incubated at 37 °C for 30 minutes. The cells were fixed on agarose pads, before visualizing on LSM510 Meta Confocal Microscope (Zeiss, Germany) using excitation wavelength of 430 nm and observing the emission of cyan fluorescence at 466 nm and yellow fluorescence at 528 nm. The FRET efficiency was measured through photobleaching of the acceptor fluorescent protein mVenus using intense pulsing of 514 nm light. The recovery of cyan emission was recorded and calculated using Equation 3 to determine the FRET efficiency.

$$E = (1 - F_{DA} / F_D) \times 100 \quad (\text{Eq. 3})$$

Where E is the FRET efficiency (%), F_{DA} is the cyan emission before mVenus photobleaching and F_D is the cyan emission after mVenus photobleaching. Each individual cell was only used once for the measurement because of the damaging effect of the photobleaching on the fluorescent proteins. The mean and standard deviations of each condition were obtained from the measurement and averaging of multiple cells (n>10). For the time-dependent experiment, the aminoglycoside antibiotic gentamicin, which is known to induce biofilm formation in *E. coli* and other bacterial cells,⁴ was used to treat the *E. coli* cells to observe the response dynamics. Photobleaching was conducted every five minutes (on different cells) upon the addition of antibiotics to the cells. Measurements were repeated five times and the mean and standard deviations were determined. Control experiments with the c-di-GMP binding VAC0042 and MrkH fused to mVenus (or mCerulean) showed insignificant changes in fluorescent intensity upon the treatment of the biofilm-dispersing compounds.

Perturbation of C-di-GMP levels in *E. coli* by biofilm-dispersing agents

Using similar protocols as described above in the antibiotic stress experiment, several biofilm dispersing compounds were tested for the perturbation of c-di-GMP levels in both the BL21 and UTI89 *E. coli* cells. The identity and concentrations of the biofilm-dispersing compounds used in this study are listed in **Table S2**. These compounds were chosen based on the reports that they are able to disperse biofilm in *E. coli* and other bacterial strains^{5,6}. Measurement of the FRET efficiencies were performed following the same protocol described above.

Perturbation of c-di-GMP levels in *E. coli* during phagocytosis in RAW264.7 murine macrophage

The RAW264.7 murine macrophage cells were cultured on petri dishes containing Dulbecco's Modified Eagle Medium (DMEM) containing high-glucose and sodium pyruvate (Hyclone, cat. no. SH30243.FS) supplemented with 10% Foetal Bovine Serum (FBS) and 100 units / mL of Penicillin-Streptomycin in 37 °C with 5% CO₂. Cells were harvested by scraping upon reaching 70 ~ 80 % confluency, and washed twice in Phosphate Buffered Saline (PBS). The cells were then resuspended into serum-free DMEM without antibiotic. The macrophage cells were allowed to adhere to glass microscope coverslips by seeding the cells onto glass coverslips submerged in DMEM without FBS and antibiotics in 6 well multi titer plates. The cells were then incubated in 37 °C with 5 % CO₂ for 3 hours before use.

Bacterial suspension of both *E. coli* BL21 and wild-type UTI89 strains were prepared as described above. The cells were spun down at 8,000 rpm for 10 minutes and washed twice in PBS. The *E. coli* cells were opsonized by resuspending in FBS, incubated at 37 °C for one hour and subsequently washed twice with PBS, before finally resuspended in serum-free DMEM without antibiotic⁷. The attached RAW264.7 cells were added with the bacterial mixture with a ratio of 1:3 of macrophage cells to bacterial cells. The suspension was incubated for 1 ~ 2 hours at 37 °C. Coverslips were then washed in cold PBS to remove excessive bacterial cells and to stop further bacterial uptake or bacterial digestion by phagolysosome. The coverslips were fixed onto a glass microscope slide and viewed over the LSM510 meta confocal microscope using settings as described above.⁸ Bacterial cells engulfed by the macrophages were compared to free swimming cells by tabulating the photobleaching profiles of more than 50 cells.

Statistical analysis

Experimental FRET efficiencies were measured by observing the change in donor emission (466 nm) upon acceptor photobleaching. The experimental results were presented as the mean or average FRET efficiencies. Statistical analysis was performed by using SigmaPlot and GraphPad software to calculate the P-values to determine the statistical significance of the observed differences in FRET efficiencies. The results are indicated by the asterisks (*, $P < 0.05$; **, $P < 0.01$; ***, $P < 0.001$).

References:

- (1) Rao, F.; Pasunooti, S.; Ng, Y.; Zhuo, W.; Lim, L.; Liu, A. W.; Liang, Z.-X. *Anal. Biochem.* **2009**, 389, 138.
- (2) Bochner, B. R.; Ames, B. N. *J. Biol. Chem.* **1982**, 257, 9759.
- (3) Schweizer, H.; Hoang, T.; Propst, K.; Ornelas, H.; Karkhoff-Schweizer, R. In *Genetic Engineering: Principles and Methods*; 2002; V 23, 69.
- (4) Hoffman, L. R.; D'Argenio, D. A.; MacCoss, M. J.; Zhang, Z.; Jones, R. A.; Miller, S. I. *Nature* **2005**, 436, 1171.
- (5) Lee, J.-H.; Cho, M. H.; Lee, J. *Environ. Microbiol.* **2011**, 13, 62.
- (6) Frei, R.; Breitbach, A. S.; Blackwell, H. E. *Angew. Chem. Inter. Ed.* 2012, 51, 5226.
- (7) Wise, A. J.; Hogan, J. S.; Cannon, V. B.; Smith, K. L. *J. Dairy Sci.* **2002**, 85, 1454.
- (8) Doyle, S. E.; O'Connell, R. M.; Miranda, G. A.; Vaidya, S. A.; Chow, E. K.; Liu, P. T.; Suzuki, S.; Suzuki, N.; Modlin, R. L.; Yeh, W.-C.; Lane, T. F.; Cheng, G. *J. Exp. Med.* **2004**, 199, 81.

Table S1 Test of the specificity of the biosensors by using the nucleotides from bacterial cells.

Nucleotide	Tested concentration	CdG-S1 biosensor			CdG-S2 biosensor		
		mVenus/mCerulean		Ratio of bound/unbound	mVenus/mCerulean		Ratio of bound/unbound
		unbound	bound		unbound	bound	
C-di-GMP	125 μM	1.56 \pm 0.01	1.01 \pm 0.02	0.65	1.38 \pm 0.01	0.87 \pm 0.01	0.63
cGMP	125 μ M	1.56 \pm 0.01	1.59 \pm 0.02	0.98	1.38 \pm 0.01	1.34 \pm 0.01	0.97
GMP	10 μ M	1.56 \pm 0.01	1.58 \pm 0.04	0.99	1.38 \pm 0.01	1.34 \pm 0.01	0.97
GDP	64 μ M	1.56 \pm 0.01	1.58 \pm 0.02	1.01	1.38 \pm 0.01	1.40 \pm 0.02	1.01
GTP	460 μ M	1.56 \pm 0.01	1.53 \pm 0.04	0.98	1.38 \pm 0.01	1.36 \pm 0.03	0.99
C-di-AMP	125 μ M	1.56 \pm 0.01	1.55 \pm 0.01	0.99	1.38 \pm 0.01	1.39 \pm 0.01	1.01
cAMP	125 μ M	1.56 \pm 0.01	1.60 \pm 0.01	1.03	1.38 \pm 0.01	1.33 \pm 0.01	0.96
AMP	125 μ M	1.56 \pm 0.01	1.61 \pm 0.05	1.03	1.38 \pm 0.01	1.33 \pm 0.02	0.96
ADP	125 μ M	1.56 \pm 0.01	1.54 \pm 0.01	0.99	1.38 \pm 0.01	1.36 \pm 0.01	0.99
ATP	1 mM	1.56 \pm 0.01	1.51 \pm 0.02	0.97	1.38 \pm 0.01	1.40 \pm 0.01	1.01
NAD ⁺	300 μ M	1.56 \pm 0.01	1.50 \pm 0.02	0.96	1.38 \pm 0.01	1.35 \pm 0.02	0.98
NADP ⁺	27 μ M	1.56 \pm 0.01	1.50 \pm 0.03	0.96	1.38 \pm 0.01	1.34 \pm 0.03	0.97

Apo-state represents the relative changes in ratio emission of sensor protein (mVenus/mCerulean) before addition of the test nucleotides.

Holo-state represents the relative changes in ratio emission of sensor protein after addition of the test nucleotides.

Ratio of Holo/Apo which is below 5 % changes are considered to be artifact

Table S2. Experimental concentrations of the biofilm-dispersing compounds and perturbation of FRET efficiencies in two *E. coli* strains.

Compound	Class	Tested concentration	BL21		UTI89	
			FRET efficiency (%)		FRET efficiency (%)	
			S1 \pm s.d.	S2 \pm s.d	S1 \pm s.d.	S2 \pm s.d
Untreated	-	-	13.6 \pm 2.4	16.5 \pm 2.0	17.8 \pm 0.8	18.2 \pm 2.5
D-Tyrosine	D – amino acid	7 μ M	13.3 \pm 1.8	17.2 \pm 1.1	14.5 \pm 3.4	14.4 \pm 3.3
N-Hexanoyl-DL homoserine lactone	AHL	25 μ M	21.0 \pm 0.9	22.9 \pm 0.2	20.0 \pm 4.8	21.2 \pm 3.7
Resveratrol	Stilbeniod	25 μ M	21.3 \pm 2.1	23.5 \pm 0.3	21.0 \pm 3.7	25.0 \pm 4.2
3-Iodolylacetonitrile	2-Aminobenzimidazole	25 μ M	23.0 \pm 1.3	24.8 \pm 1.2	23.3 \pm 2.0	23.2 \pm 1.6
MAHMA-NONOate	NO donor	100 μ M	21.6 \pm 0.8	23.6 \pm 0.6	22.8 \pm 4.4	24.4 \pm 3.5

AHL: N-Acyl homoserine lactone

NO: Nitric oxide

Table S3. Minimal inhibition concentration (MIC), experimental concentrations of the antibiotics and perturbation of FRET efficiencies in two *E. coli* strains.

Antibiotic	Class	MIC 90% ($\mu\text{g/mL}$)	Tested concentration ($\mu\text{g/mL}$)	BL21		UTI89	
				FRET efficiency (%)		FRET efficiency (%)	
				S1 \pm s.d.	S2 \pm s.d	S1 \pm s.d	S2 \pm s.d
Untreated	-	-	-	18.9 ± 2.3	19.4 ± 2.6	18.0 ± 2.5	18.2 ± 2.5
Gentamicin	Aminoglycoside	8-10	3	2.3 ± 1.9	10.1 ± 2.9	7.8 ± 1.5	10.4 ± 4.4
Streptomycin		12-20	3	2.0 ± 1.7	10.1 ± 4.9	7.5 ± 1.7	12.2 ± 1.7
Tobramycin		16	3	8.0 ± 2.2	13.5 ± 0.6	8.8 ± 1.6	11.5 ± 1.6
Erythromycin	Macrolide	8	0.6	2.2 ± 0.30	15.0 ± 1.0	8.6 ± 2.3	16.3 ± 4.8
Ampicillin	Beta-lactam	8	5	7.2 ± 2.20	17.2 ± 2.0	12.8 ± 2.6	15.5 ± 1.7
Norfloxacin	Quinolones	8	0.25	15.0 ± 0.3	18.6 ± 1.2	15.8 ± 2.1	17.5 ± 2.2
Mitomycin C	Aziridine	-	50	16.7 ± 1.3	18.1 ± 3.9	15.8 ± 2.6	16.9 ± 2.4
Vancomycin	Glycopeptide	4	1	3.0 ± 0.02	3.6 ± 0.2	5.7 ± 1.8	6.4 ± 3.2

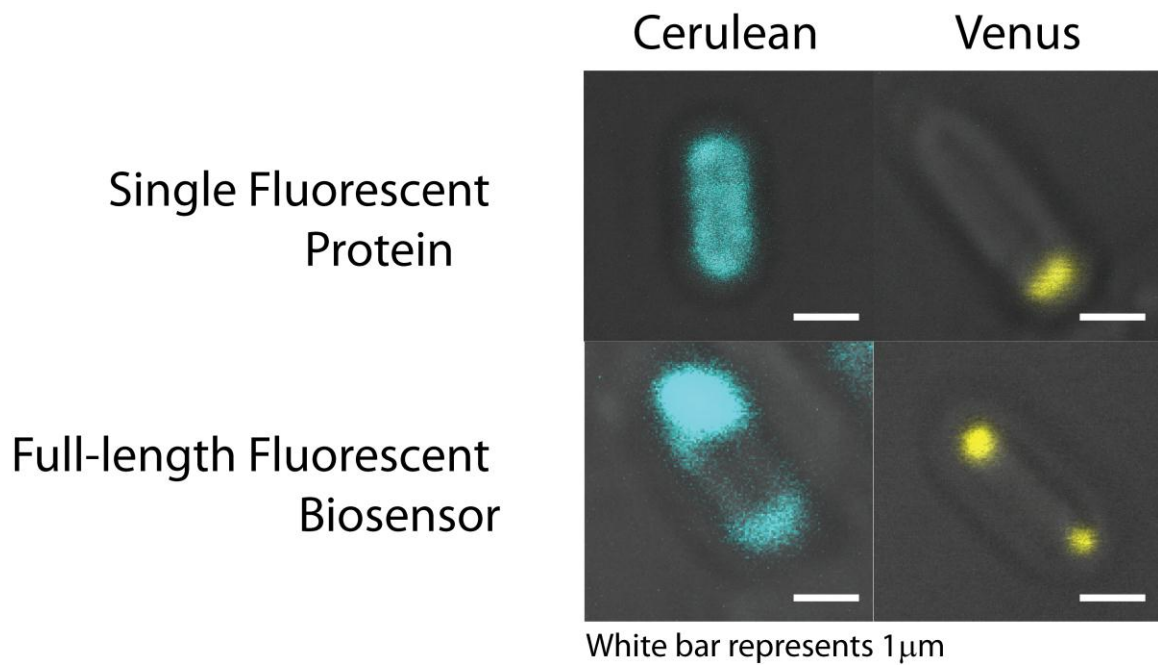


Fig. S1. Polar localization of mCerulean, mVenus and Cdg-S2 in BL21 *E. coli* cells. Both the CFP and YFP channels are shown. mVenus has a greater tendency to localize at the poles than mCerulean.

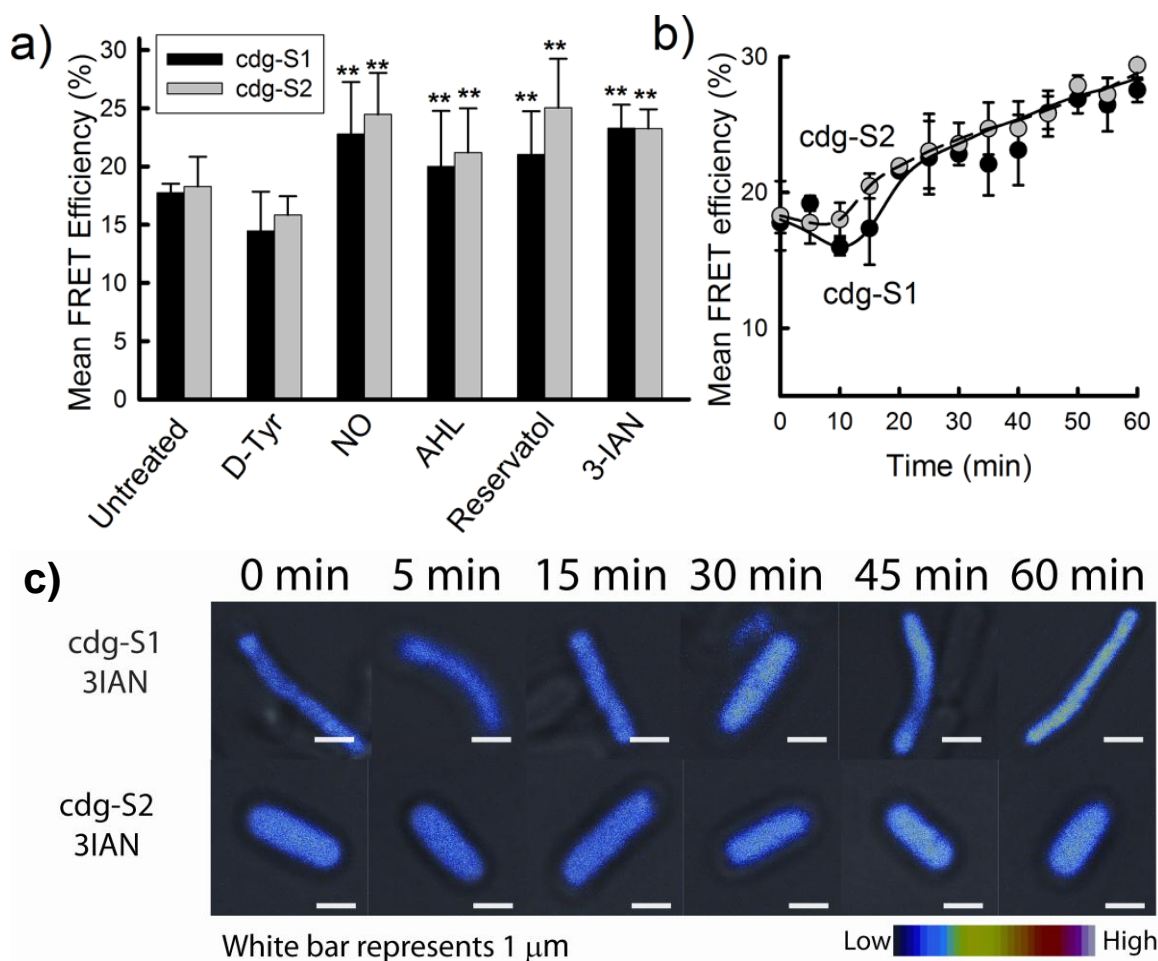


Fig. S2. Perturbation of c-di-GMP levels in UT189 *E. coli* cells by biofilm-dispersing agents. a) Average FRET efficiencies for the *E. coli*-containing biosensors before and after the treatment with biofilm-dispersing agents for 30 min. FRET efficiency was measured by observing the change in donor emission (466 nm) upon acceptor photobleaching (see Supporting Information). Statistical significance is indicated by the asterisk (*, $P < 0.05$; **, $P < 0.01$). Changes in FRET efficiency are directly correlated to changes in the population of ligand binding biosensors and thus to c-di-GMP level. b) Time-dependent change of the FRET efficiencies for 3-IAN-treated cells. c) Representative images of YFP (λ_{430} nm excitation, λ_{528} nm emission) prior to acceptor photobleaching.

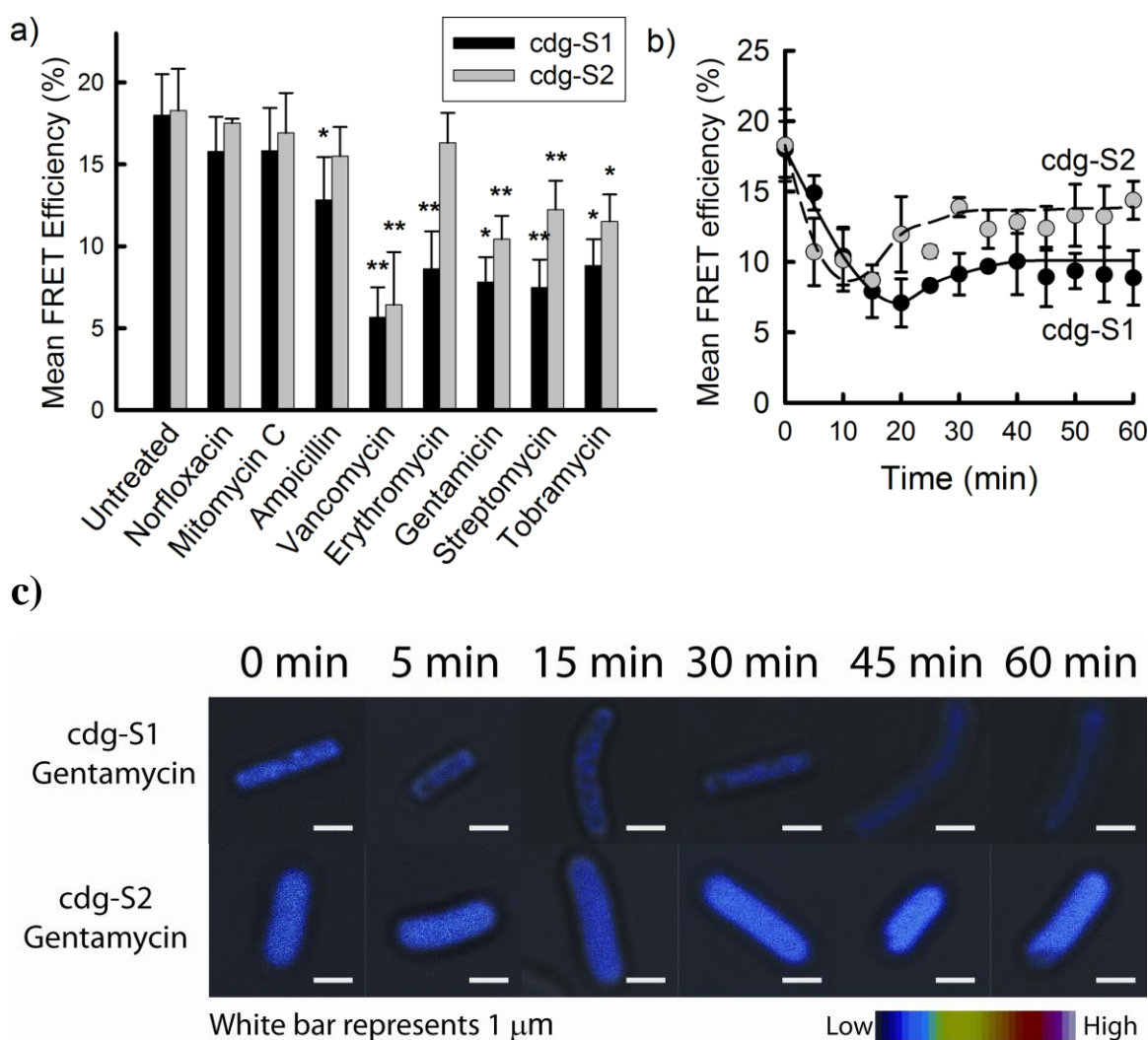
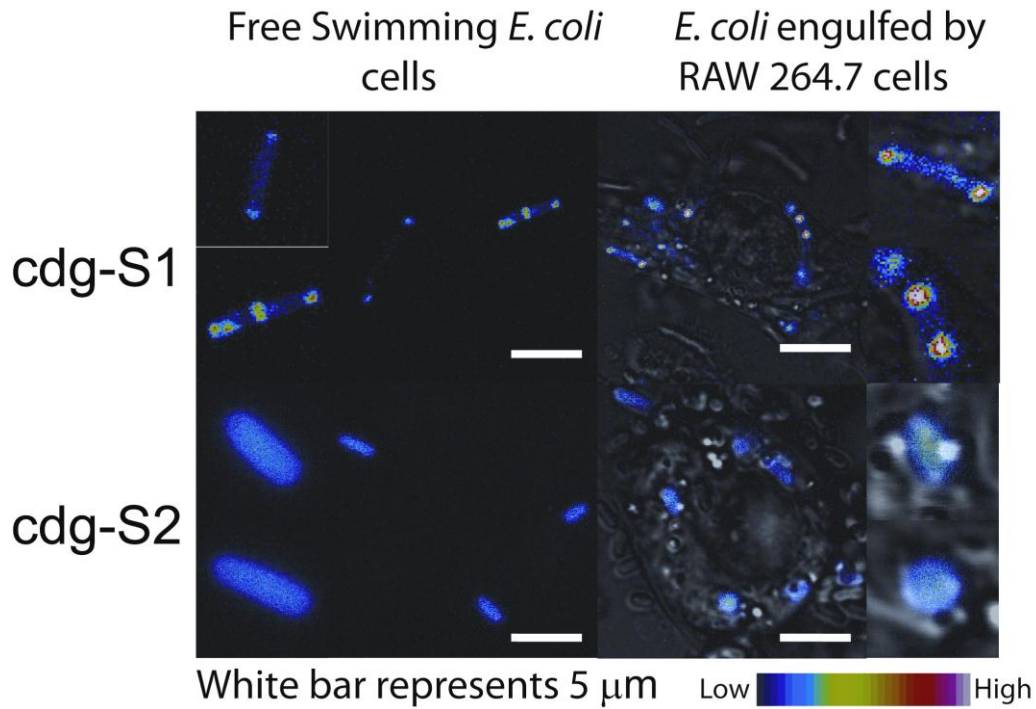
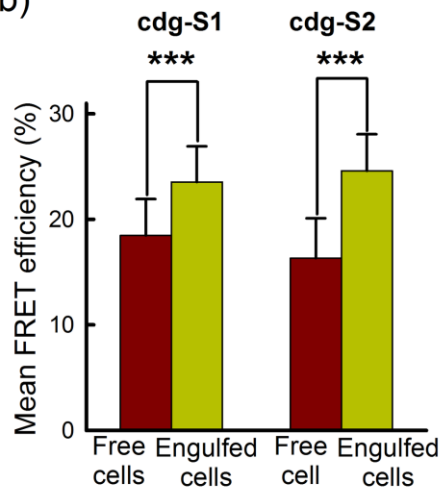


Fig. S3. Perturbation of c-di-GMP levels in UT189 *E. coli* cells by subinhibitory concentration antibiotics. a) Average FRET efficiencies for the *E. coli*-containing biosensors before and after the treatment with antibiotics for 30 min. FRET efficiency was measured by observing the change in donor emission (466 nm) upon acceptor photobleaching (see Supporting Information). Statistical significance is indicated by the asterisk (*, $p < 0.05$; **, $P < 0.01$). Data were obtained by averaging the readings for multiple cells ($n > 10$). Changes in FRET ratio are directly correlated to changes in the population of ligand binding biosensors and thus to c-di-GMP level. b) Time-dependent change of the FRET efficiencies for gentamycin. c) Representative images of YFP ($\lambda 430$ nm excitation, $\lambda 528$ nm emission) prior to acceptor photobleaching.

a)



b)



c)

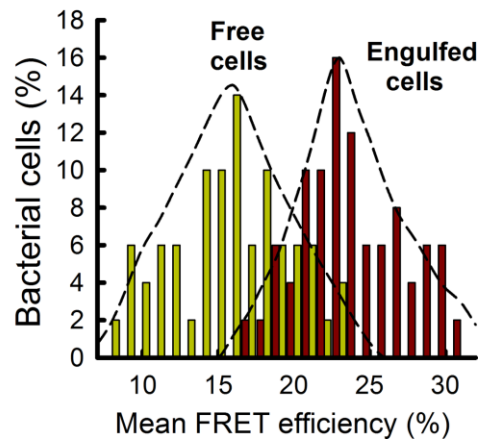


Fig. S4. Perturbation of c-di-GMP level in the UT189 *E. coli* cells engulfed by macrophage. a) Representative images of YFP ($\lambda 430$ nm excitation, $\lambda 528$ nm emission) prior to acceptor photobleaching of the *E. coli* cells outside and inside of RAW264.7 macrophage cells. Side panels show the enlarged views of the bacterial cells. b) Average FRET efficiencies for the *E. coli* cells outside and inside of the macrophage. Statistical significance is indicated by the asterisk (***, $P < 0.001$). c) Histogram showing the FRET efficiency distribution for cdgS2 in the free and macrophage-engulfed *E. coli* cells. (Total number of cells are 50 (free) and 53 (engulfed))